Stem Cell Reports
Article

ISSCR

OPEN ACCESS

Development and Characterization of a Human and Mouse Intestinal Epithelial Cell Monolayer Platform

Kenji Kozuka,[1] Ying He,[1] Samantha Koo-McCoy,[1] Padmapriya Kumaraswamy,[1] Baoming Nie,[1] Karen Shaw,[1] Priscilla Chan,[1] Michael Leadbetter,[1] Limin He,[1] Jason G. Lewis,[1] Ziyang Zhong,[1] Dominique Charmot,[1] Marwan Balaa,[2] Andrew J. King,[1] Jeremy S. Caldwell,[1] and Matthew Siegel[1,*]

[1]Ardelyx, Inc., 34175 Ardenwood Boulevard, Suite 200, Fremont, CA 94555, USA
[2]Endoscopy Center of Silicon Valley, 2410 Samaritan Drive, Suite 100, San Jose, CA 95124, USA
*Correspondence: msiegel@ardelyx.com
https://doi.org/10.1016/j.stemcr.2017.10.013

SUMMARY

We describe the development and characterization of a mouse and human epithelial cell monolayer platform of the small and large intestines, with a broad range of potential applications including the discovery and development of minimally systemic drug candidates. Culture conditions for each intestinal segment were optimized by correlating monolayer global gene expression with the corresponding tissue segment. The monolayers polarized, formed tight junctions, and contained a diversity of intestinal epithelial cell lineages. Ion transport phenotypes of monolayers from the proximal and distal colon and small intestine matched the known and unique physiology of these intestinal segments. The cultures secreted serotonin, GLP-1, and FGF19 and upregulated the epithelial sodium channel in response to known biologically active agents, suggesting intact secretory and absorptive functions. A screen of over 2,000 pharmacologically active compounds for inhibition of potassium ion transport in the mouse distal colon cultures led to the identification of a tool compound.

INTRODUCTION

The intestinal epithelium is composed of a single layer of polarized columnar epithelial cells with a diverse range of functions, including acting as a barrier to separate the intestinal luminal contents and microbes from the underlying tissue, controlling the absorption of nutrients and the excretion of waste, secreting hormones for paracrine and endocrine signaling, and communicating with the underlying gut-associated lymphoid tissue (Furness et al., 1999). The gene and protein expression patterns of this epithelium vary along the longitudinal axis of the intestine to reflect the functional role of the different intestinal segments. For example, the abundance of bicarbonate transporters expressed in the duodenum is consistent with the neutralization of acidic chyme entering from the stomach (Seidler et al., 2011). Similarly, the abundance of digestive brush border enzymes and nutrient transporters in the jejunum, bile acid transporters in the ileum, and electrolyte transporters in the colon is consistent with the nutrient digestion and assimilation role of the jejunum, the bile acid reabsorption role of the ileum, and the water and electrolyte reabsorption role of the colon, respectively (Daniel, 2004; Dawson et al., 2009; Kunzelmann and Mall, 2002).

Minimally systemic drugs that target and modulate these intestinal epithelial functions exert their pharmacological activity with little or no systemic absorption, thereby minimizing unnecessary exposure of other organ systems to the drug and reducing the potential for side effects (Charmot, 2012). Development of an intestinal epithelial cell culture system could help to accelerate the discovery and development of drugs that target the gastrointestinal epithelium by facilitating structure-activity relationship optimization, mechanism-of-action studies, new target identification, and drug permeability measurements in the native cell type expressing endogenous drug targets. Moreover, development of both rodent and human intestinal epithelial cell cultures to evaluate drug candidates could help to reduce translational risk before initiating clinical studies. However, traditional cell culture models of the intestine use cancer cell lines, such as Caco-2, which contain unknown mutations and which, although derived from the colon, may not accurately represent any one segment of the gut or its diverse cell lineages (Sun et al., 2008).

Intestinal organoids, or enteroids, are three-dimensional intestinal epithelial cell cultures maintained by a set of growth factors that simulate the intestinal stem cell niche (Jung et al., 2011; Sato et al., 2009, 2011). Cultures from the mouse small intestine bud crypt-like structures containing intestinal stem cells, Paneth cells, and transit-amplifying cells, while cells close to the pseudo-lumen are differentiated into absorptive and secretory cell lineages (Sato et al., 2009). Mouse colon and human intestinal organoids are maintained by the addition of exogenous Wnt protein and can be differentiated into absorptive and secretory cell lineages by removing Wnt and other factors that prevent cell differentiation (Jung et al., 2011; Sato et al., 2011). Intestinal organoids recapitulate gastrointestinal epithelial cell biology, gene expression, and function, and have provided an invaluable resource for exploring

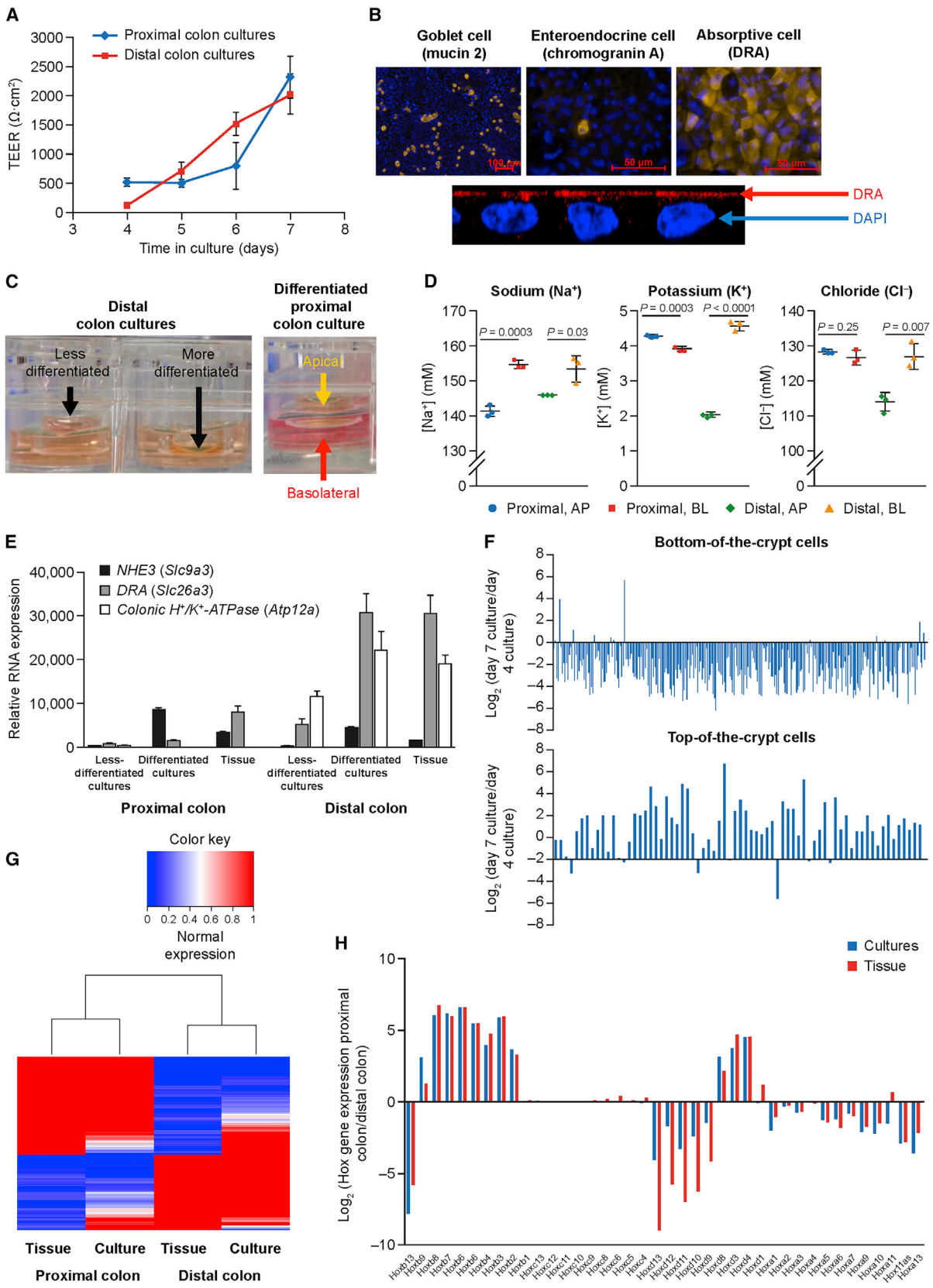

(legend on next page)

fundamental intestinal cellular and molecular biology (Farin et al., 2016; Grun et al., 2015; Middendorp et al., 2014). Cells derived from intestinal organoids can be transplanted *in vivo*, where they are able to integrate into intestinal tissue with no functional or histological abnormalities (Yui et al., 2012). However, there are only a few published examples of the use of intestinal organoids in the development of functional assays to screen pharmacological compounds (Dekkers et al., 2013; van de Wetering et al., 2015).

A distinct limitation of three-dimensional organoids for use in drug discovery is that the apical membrane faces the inside of the organoid. This enclosed architecture results in the accumulation of dead cells and mucus inside the organoid lumen, which creates a diffusion barrier and requires microinjection for luminal drug administration and transport studies, thereby limiting throughput and utility. To make intestinal organoids more suitable for assay development and functional evaluation, methods have been developed for converting intestinal epithelial organoids into monolayer cultures (In et al., 2016; Moon et al., 2014; VanDussen et al., 2015). Although these cultures polarize, form tight junctions, and differentiate into the major intestinal cell lineages, the characterization of these cultures to date has been limited, only monitoring a handful of intestinal cell lineage and differentiation markers, and providing no comparison with endogenous expression levels in native tissue. No consensus has been reached for optimal culture growth and differentiation conditions, and different methods for human monolayer growth and differentiation have been published (In et al., 2016; VanDussen et al., 2015).

Here, we establish robust and reproducible monolayer growth conditions optimized for all segments of the mouse and human small and large intestines on a scale suitable for detailed investigations of epithelial cell biology, translational drug discovery, compound screening, and mechanism-of-action studies. Culture conditions were optimized by comparing segment-specific global gene expression patterns of the monolayers with those of freshly isolated intestinal tissue, by the evaluation of trans-epithelial electrical resistance (TEER), and through characterization of the ion transport phenotype. The technology was miniaturized into 96-well plates to support high-throughput compound screening. Application of this platform to drug discovery is demonstrated by the identification of an inhibitor of active potassium ion (K^+) absorption in the mouse distal colon via a phenotypic screen using a library of approximately 2,000 bioactive compounds, providing a lead to further develop for the treatment of hyperkalemia.

RESULTS

Establishment and Evaluation of Mouse Colon Monolayer Cultures

To establish cell cultures from the mouse intestine we used freshly isolated crypts to minimize the likelihood of changes that may occur upon *ex vivo* culture and owing to the availability of robust protocols for intestinal crypt isolation (Gracz et al., 2012). Initial attempts at establishing monolayer cultures were with the growth factor combination used for three-dimensional mouse colon organoids, i.e., Wnt3a, epidermal growth factor (EGF), noggin, and R-spondin 1 (WENR). Using WENR growth media, mouse colon cultures achieved confluence and yielded increasing TEER over time, suggesting the formation of tight junctions. Although cultures spontaneously differentiated upon forming a confluent monolayer, presumably due to contact inhibition, removal of Wnt3a and R-spondin1

Figure 1. Development and Characterization of Mouse Colon Monolayer Cultures

(A) TEER of proximal and distal colon cultures over time. Mean ± SD, n = 12. Representative of at least three experiments.

(B) Upper images, immunostaining for major cell lineages of the colon cultures; lower image, confocal microscopy z stack image showing apical localization of DRA (SLC26A3) relative to the cell nucleus (DAPI staining). Representative of at least three experiments.

(C) Cultures grown on Transwells showing absorption of water from the apical compartment to the basolateral compartment in distal colon cultures, and apical secretion of acid in proximal colon cultures (phenol red dye: yellow indicates acidic pH; pink indicates neutral pH). Representative of at least three experiments.

(D) Ion chromatography analysis of medium in the apical and basolateral compartments of proximal and distal colon cultures. Mean ± SD, n = 3. Data representative of at least two experiments.

(E) Comparison of RNA expression patterns of ion transporters in proximal and distal colon cultures and tissue. Mean ± SD, average of two replicate experiments with triplicate wells.

(F) Comparison of gene expression patterns of differentiated distal colon (day 7) versus less-differentiated distal colon (day 4) cultures with lists representing the most differentially expressed genes from less-differentiated (bottom-of-the-crypt) and more differentiated (top-of-the-crypt) colon cells, sorted by EPHB2 expression.

(G) Heatmap comparing gene expression in cultures with tissue for genes with at least 5-fold differential expression between the proximal colon tissue and distal colon tissue (see Table S1).

(H) Differential expression of the Hox gene family in the mouse proximal versus distal colon for differentiated cultures and colon tissue. AP, apical; BL, basolateral; TEER, trans-epithelial electrical resistance.

accelerated differentiation, and TEER exceeded 2,000 $\Omega \cdot cm^2$ under these conditions (Figure 1A).

Immunostaining the cultures for markers of the major cell lineages in the mouse colon confirmed differentiation into absorptive, goblet, and enteroendocrine cell lineages (Figure 1B). Confocal microscopy imaging confirmed cell polarization based on the apical localization of the chloride (Cl^-)/bicarbonate ion transporter DRA (SLC26A3) relative to the cell nucleus (Figure 1B).

After differentiation, mouse distal colon cultures showed a phenotype characterized by rapid absorption of water from the apical compartment into the basolateral compartment (Figure 1C). In contrast, differentiated mouse proximal colon cultures showed less water absorption compared with distal colon cultures but, instead, displayed an apically directed acid-secretion phenotype as demonstrated by a yellow color of pH-sensitive phenol red dye in the apical medium (indicating acidic pH) and a pink color in the basolateral medium (indicating neutral pH) (Figure 1C). Ion chromatography analysis of the media in both compartments showed net Na^+, K^+, and Cl^- absorption from the apical compartment into the basolateral compartment in the distal colon cultures, but only net Na^+ absorption in the proximal colon cultures (Figure 1D).

Taken together, the phenotype and ion transport measurements of the colon cultures are consistent with known functional ion transport and ion transporter expression patterns of NHE3 (SLC9A3), DRA (SLC26A3), and the colonic H^+/K^+-ATPase (ATP12A) in the mouse colon (Talbot and Lytle, 2010; Sangan et al., 1997). To confirm the expression pattern of these transporters, global transcript expression was obtained using RNA sequencing from freshly isolated colon crypts, less-differentiated mouse colon cultures (taken on day 4), and more differentiated colon cultures (taken on day 7). Expression patterns of *NHE3*, *DRA*, and *colonic H^+/K^+-ATPase* in the differentiated monolayer cultures were consistent with freshly isolated colon tissue and with the observed ion transport phenotype. *NHE3* was expressed in both proximal and distal colon cultures and *DRA* and *colonic H^+/K^+-ATPase* showed higher expression levels in the distal than in the proximal colon cultures (Figure 1E). Furthermore, these ion transporter genes were upregulated upon culture differentiation, which is consistent with their increased expression in differentiated colonocytes localized on the surface of the colon (Talbot and Lytle, 2010; Sangan et al., 1997).

Differential gene expression patterns in day 4 versus day 7 mouse colon cultures were compared with previously reported lists representing the most differentially expressed genes from less-differentiated (bottom-of-the-crypt) and more differentiated (top-of-the-crypt) colon cells isolated from tissue, sorted based on EPHB2 expression (Merlos-Suarez et al., 2011). The results suggest that the gene expression pattern in day 4 mouse colon cultures is consistent with less-differentiated colon cells, while the gene expression pattern in day 7 colon cultures is consistent with more differentiated colon cells (Figure 1F).

RNA sequencing was used to evaluate whether the cultures maintained segment-specific gene expression patterns by comparing the expression of genes with at least 5-fold differential expression between mouse proximal and distal colon tissues to the relative expression of these genes in the monolayer cultures (Table S1). The cultures clustered unsupervised with the intestinal tissue segment of origin, and relative gene expression patterns in the cultures were similar to those in the corresponding tissue segments (Figure 1G). *Hox* genes, which encode transcription factors critical for embryonic development, were well represented in the list of genes differentially expressed in freshly isolated tissue from the proximal versus distal colon. Therefore, the differential expression of all *Hox* genes comparing proximal with distal colon was evaluated and observed to be similar in the monolayer cultures relative to fresh tissue (Figure 1H).

Establishment and Evaluation of Mouse Small Intestine Monolayer Cultures

Unlike mouse colon cultures, mouse jejunum monolayer cultures were unable to grow to confluence in either the standard three-dimensional organoid medium using EGF, noggin, and R-spondin 1 (ENR medium) or the mouse colon culture condition using WENR medium. Two modifications of the mouse colon culture conditions were necessary for the cells to grow to confluence reproducibly. First, the rho-associated protein kinase inhibitor Y-27632 (Y), which is typically added only for the first 2 days after seeding the cells to minimize anoikis, was required throughout the duration of the culture. Secondly, Wnt3a concentration needed to be increased from the standard concentration of 100 ng per mL; 250 ng per mL was chosen as a concentration that reproducibly produced confluent cultures with acceptable TEER.

Despite achieving confluence, the mouse jejunum cultures, unlike the colon, did not display a strong functional phenotype, and it was unclear whether these cultures represented well-differentiated villus-like cells or less-differentiated crypt-like cells. Therefore, global gene expression by RNA sequencing was obtained for 36 culture conditions with varying concentrations of Wnt3a, taken 4, 6, and 8 days after seeding the cultures, and compared with the gene expression profiles of mouse jejunum villi and crypts. To simplify analysis and to account for changes in global gene expression rather than relying on a handful of marker genes, the Pearson correlation coefficient was calculated for the relationship between the entire gene expression profiles of cultured monolayer cells and of freshly isolated

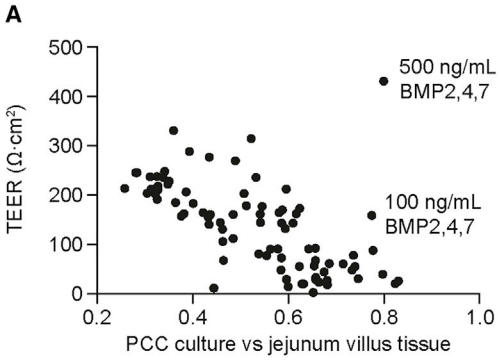

B

Growth factors	PCC jejunum culture vs jejunum villus tissue	PCC jejunum culture vs jejunum crypt tissue
ET + 300 ng/mL BMP2	0.69	0.41
ET + 300 ng/mL BMP4	0.71	0.50
ET + 300 ng/mL BMP7	0.61	0.63
ET + 100 ng/mL BMP2	0.71	0.52
ET + 100 ng/mL BMP4	0.63	0.63
ET + 100 ng/mL BMP7	0.51	0.71
ET + 30 ng/mL BMP2	0.50	0.66
ET + 30 ng/mL BMP4	0.48	0.72
ET + 30 ng/mL BMP7	0.47	0.74
ET + 10 ng/mL BMP2	0.49	0.74
ET + 10 ng/mL BMP4	0.46	0.75
ET	0.46	0.76

C

Culture		Duodenum villus tissue	Jejunum villus tissue	Ileum villus tissue
Duodenum	ET	0.56	0.51	0.49
	ET + 100 ng/mL BMP2	0.69	0.54	0.44
	ET + 300 ng/mL BMP4	0.74	0.60	0.43
	ET + 100 ng/mL BMP2,4	0.73	0.60	0.44
Jejunum	ET	0.54	0.58	0.53
	ET + 100 ng/mL BMP2	0.79	0.82	0.55
	ET + 300 ng/mL BMP4	0.79	0.82	0.51
	ET + 100 ng/mL BMP2,4,7	0.78	0.81	0.47
Ileum	ET	0.42	0.48	0.56
	ET + 100 ng/mL BMP2	0.58	0.65	0.65
	ET + 300 ng/mL BMP4	0.58	0.65	0.66
	ET + 100 ng/mL BMP2,4,7	0.58	0.64	0.59

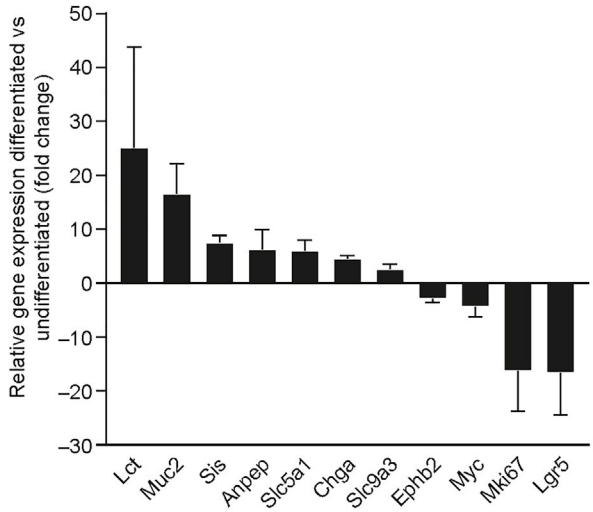

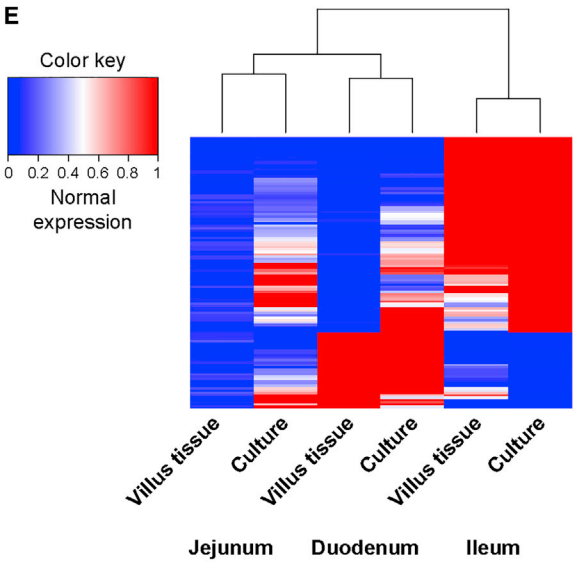

Figure 2. Development and Characterization of Mouse Small Intestine Monolayer Cultures

(A) Plot of Pearson correlation coefficients (PCC) comparing global gene expression in jejunum cultures versus jejunum villus tissue against TEER for jejunum cultures grown under various conditions.

(B) PCC for global gene expression in jejunum cultures versus jejunum villus or crypt tissue differentiated with varying concentrations of BMP-2, BMP-4, or BMP-7.

(legend continued on next page)

mouse jejunum villus cells. Use of the Pearson correlation coefficient as a quantitative measurement of similarity was verified by comparing the correlation coefficients for the expression profiles of genes that are markers of either undifferentiated cells (*Lgr5*, *Ephb2*) or differentiated cells (lactase [*Lct*], sucrase-isomaltase [*Sis*], Sglt1 [*Slc5a1*], DPP IV [*Dpp4*], and NHE3 [*Slc9a3*]). The resulting strong negative correlation with undifferentiated cell markers and positive correlation with differentiated cell markers validated this approach of optimizing growth conditions for differentiated small intestinal cultures (Figure S1).

Although the expression profiles of several samples from day 8 in this initial dataset showed a strong correlation with mouse jejunum villi gene expression (Pearson correlation coefficient up to approximately 0.8), these cultures showed visual gaps in the monolayer and their TEER was near background levels despite reaching confluence and having high TEER earlier in the culture. Therefore, a second set of gene expression data using 48 culture conditions was obtained in which measures were taken to try to differentiate the culture rapidly upon reaching confluence. A panel of small-molecule Wnt pathway inhibitors and a mixture of bone morphogenetic proteins (BMPs) 2, 4, and 7 were among the conditions tested. Plotting the Pearson correlation coefficient against TEER for these 48 samples along with the 36 samples from the previous experiment confirmed the trend of reduced TEER in cultures that had the highest correlation with jejunum villi, except for the cultures treated with either 100 or 500 ng per mL BMPs 2, 4, and 7, which both showed a strong correlation with jejunum villi gene expression and maintained monolayer integrity (Figure 2A).

Dose titration of individual BMPs indicated that 100 ng per mL BMP-2 and 300 ng per mL BMP-4 resulted in cultures that had strong correlations of gene expression with villus tissue in the jejunum and ileum and were as effective as the BMP mixture at differentiating mouse duodenum, jejunum, and ileum cultures (Figures 2B and 2C; Table S2). Cultures differentiated with sub-optimal concentrations of BMPs, or in the absence of BMPs, showed stronger correlation with freshly isolated jejunum crypts, suggesting that these cultures maintain a less-differentiated phenotype (Figure 2B; Table S2). Comparing a panel of differentiation marker genes from day 4 cultures with day 7 cultures differentiated with BMP-4 showed upregulation of gene markers for mature enterocytes, goblet cells, and enteroendocrine cells, and a downregulation of gene markers for proliferation and intestinal stem cells (Figure 2D).

We chose 300 ng per mL BMP-4, combined with EGF and thiazovivin, as the preferred small intestine differentiation condition. Under these conditions, the Pearson correlation coefficients for small intestinal cultures were highest for the segment from which the cultures were derived (Figure 2C). Many of the genes that show segment-specific expression in intestinal tissue showed similar expression patterns in the cultures and, as a result, the cultures clustered unsupervised with the intestinal tissue segment of origin (Figure 2E; Table S3). Immunostaining for cell-specific markers confirmed that cells from absorptive, goblet, enteroendocrine, and Paneth cell lineages were present in the differentiated cultures (Figure 3A). Quantification of lineage marker gene expression was consistent with the presence of all major cell lineages in the small intestine and colon cultures, although the expression levels of *Muc2* were lower in cultures relative to the corresponding tissue (Figure S2).

Ion transport analysis of Na^+, K^+, Cl^-, and phosphate (PO_4) showed net Na^+ absorption and apically directed acid secretion in the small intestinal cultures, consistent with NHE3 expression throughout the small intestine (Figures 3B, 3C, and 3D). PO_4 was actively absorbed only in the ileum culture (Figures 3C and 3D), consistent with the exclusive expression of the Na^+/PO_4 co-transporter NaPi2b (SLC34A2) in the mouse ileum (Sabbagh et al., 2009). K^+ and Cl^- ion concentrations were higher on the apical side than the basolateral side, but when the change in apical volume was accounted for (apical volume decreases with time), both K^+ and Cl^- showed net absorption in the mouse small intestinal cultures (Figures 3C and 3D). Overall, the net absorption of Na^+, K^+, and Cl^- ions in the mouse jejunum and ileum cultures, and the active absorptive transport of PO_4 only in the mouse ileum, are consistent with the *in vivo* function of these segments.

Establishment and Evaluation of Human Intestine Monolayer Cultures

Owing to the limited availability of fresh human intestinal tissue, human intestine monolayer cultures were developed using cells derived from three-dimensional human

(C) PCCs for global gene expression in duodenum, jejunum, and ileum cultures versus villus tissue for different intestinal segments.
(D) Relative gene expression in BMP-4-differentiated jejunum cultures versus undifferentiated (day 4) jejunum cultures for marker genes of differentiated (*Lct, Muc2, Sis, Anpep, Slc5a1, Chga,* and *S.lc9a3*) and undifferentiated (*Ephb2, Myc, Mki67*, and *Lgr5*) small intestine epithelial cells. Average of two replicate experiments with triplicate wells. Mean ± SD.
(E) Heatmap comparing gene expression in cultures versus tissue for duodenum, jejunum, and ileum using a list of genes with intestinal segment-specific expression (more than 5-fold enriched villus expression relative to the other intestinal segments; see Table S3).
BMP, bone morphogenetic protein; E, epidermal growth factor; T, thiazovivin; TEER, trans-epithelial electrical resistance.

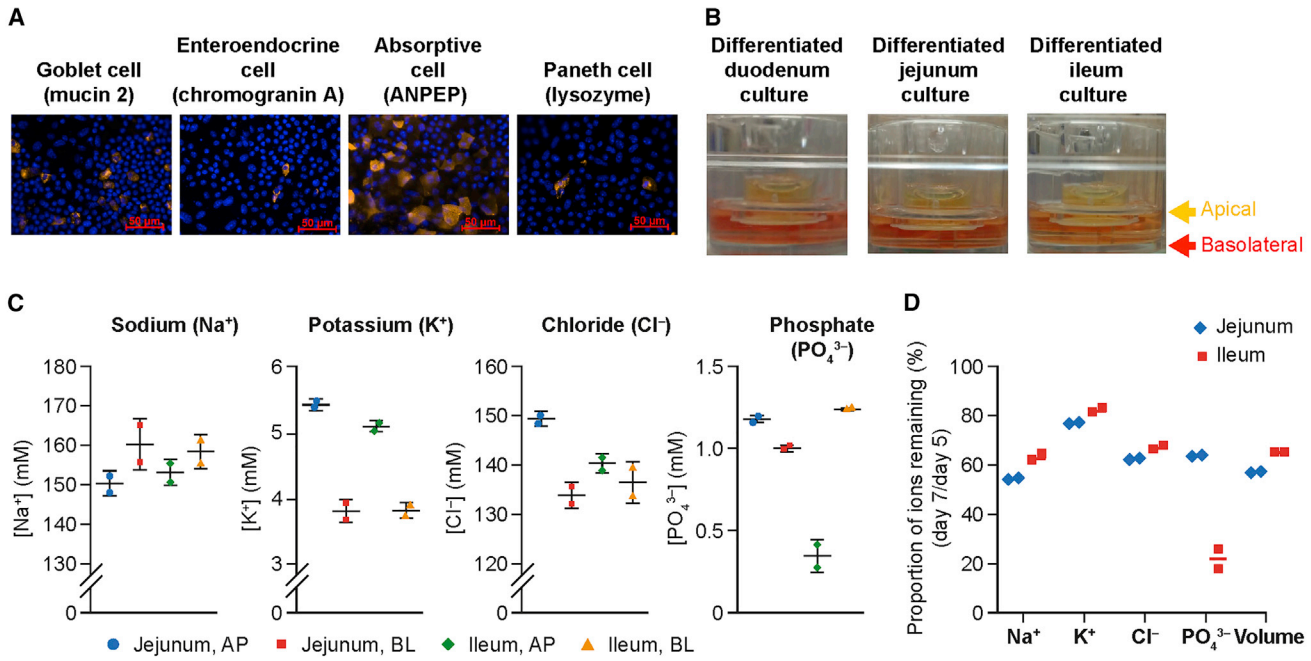

Figure 3. Phenotype of Mouse Small Intestine Monolayer Cultures

(A) Immunostaining for major cell lineages in jejunum cultures.

(B) pH analysis of medium in the apical and basolateral compartments for cultures from duodenum, jejunum, and ileum (phenol red dye: yellow indicates acidic pH; pink indicates neutral pH).

(C) Ion concentrations in the apical and basolateral compartments of jejunum and ileum cultures 2 days after differentiation. Mean ± SD, n = 2. Representative of at least two experiments.

(D) Total ion amount (concentration × volume) in the apical compartment of mouse jejunum and ileum cultures on day 7 relative to day 5 when fresh differentiation medium was added. Representative of at least two independent experiments.

ANPEP, aminopeptidase N; AP, apical; BL, basolateral.

intestinal organoids, which requires the addition of nicotinamide (Nic), transforming growth factor β (TGF-β) receptor signaling inhibitor (A83-01 [A]), and a p38 inhibitor (SB202190 [S]) to WENR medium (WENRNicAS) for long-term growth (Sato et al., 2011). Human cultures were established using biopsies from the duodenum, terminal ileum, and ascending, transverse, descending, and sigmoid colon.

To optimize growth conditions, monolayer cultures from the human distal colon were chosen using the water-absorption phenotype characteristic of this segment as the readout. Inclusion of A83-01 was necessary for proper differentiation of water-absorbing cultures (Figure S3). Substitution of Y-27632 with thiazovivin in the seeding medium resulted in human colon cultures that had higher TEER, while maintaining similar global transcriptional profiles, although thiazovivin resulted in some suppression of secretory cell differentiation (Figures S4 and S5). Distal colon cultures seeded in WENRAT or WENRNicAST media and differentiated with ENRA, ENA, or A83-01 media consistently yielded absorptive cultures that showed active transport of Na^+, K^+, and Cl^- (Figure 4A), and global RNA sequencing indicated that cultures grown under these two conditions were strongly correlated (Figure S4). However, the inclusion of Nic and SB202190 in the WENRNicAST seeding medium further suppressed differentiation of secretory cells in human colon cultures, and so seeding with WENRAT followed by differentiation with ENRA was chosen as the standard medium combination (Figure S5).

Immunostaining for cell lineage markers showed that all major cell types of the colon were present in the human cultures (Figure 4B). Analysis of ion transporter expression showed patterns similar to those observed in the mouse, with *NHE3* and *DRA* expressed in both proximal and distal colon cultures, and *colonic H^+/K^+-ATPase* (*ATP12A*) expression restricted to the distal colon cultures (Figure 4C). While *NHE3* and *DRA* expression levels in the cultures were similar to those in tissue, *colonic H^+/K^+-ATPase* expression was much higher in distal colon cultures than in human distal colon tissue (Figure 4C). Using day 3 cultures grown in WENRNicAST medium as a less-differentiated condition, comparing a panel of marker genes with optimized day 6 differentiated cultures showed that genes characteristic of mature surface colonocytes, goblet cells, and enteroendocrine cells were upregulated following

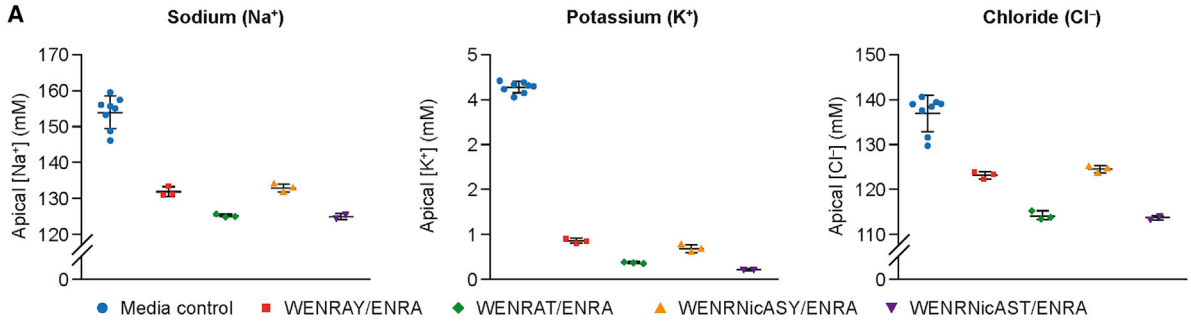

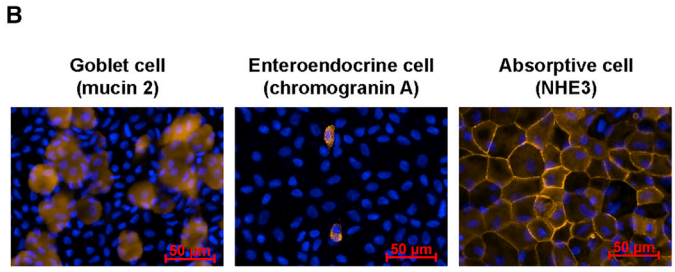

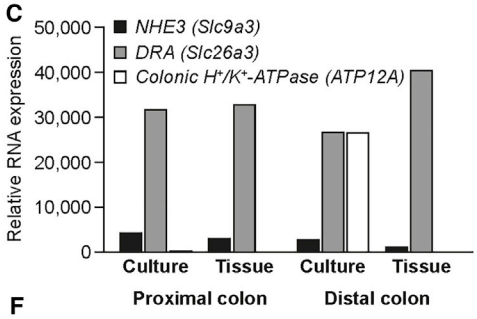

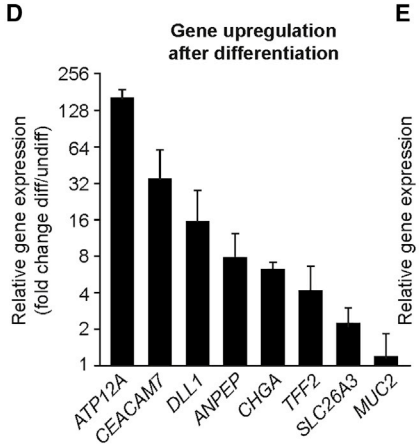

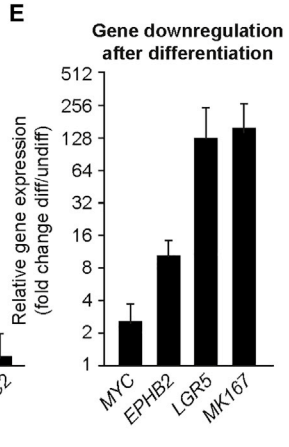

F

Patient 13 duodenum culture conditions	Patient 11 tissue	Patient 13 tissue
WENRAY day 3	0.48	0.58
WENRAY/ENRA day 6	0.57	0.65
WENRAY/ENA day 6	0.77	0.81
WENRAY/A day 6	0.79	0.83
Patient 11 tissue	1.00	0.93
Patient 13 tissue	0.93	1.00

Patient 11 duodenum culture conditions	Patient 11 tissue	Patient 13 tissue
WENRAY day 3	0.44	0.52
WENRAY/ENRA day 6	0.61	0.65
WENRAY/ENA day 6	0.77	0.80
WENRAY/A day 6	0.75	0.79
Patient 11 tissue	1.00	0.93
Patient 13 tissue	0.93	1.00

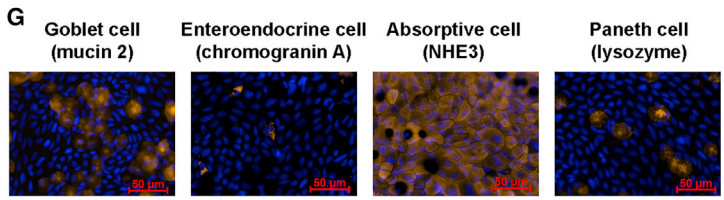

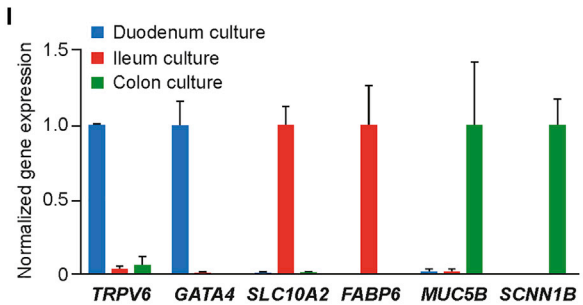

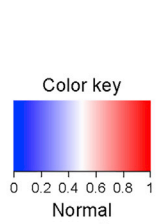

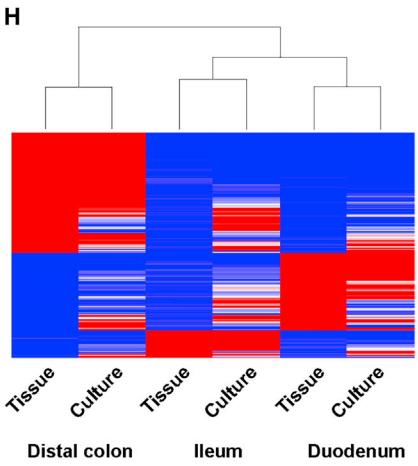

(legend on next page)

differentiation while marker genes of less-differentiated intestinal cells were down-regulated after differentiation (Figures 4D and 4E). Optimal growth conditions for the human colon were successfully applied to different colonic segments in six different patients, suggesting that these growth conditions were not patient-specific.

Initial attempts at growing human duodenum and ileum cultures focused on seeding in WENRAY, WENRAT, WENRNicASY, and WENRNicAST media, and differentiating with ENRA medium. However, duodenum cultures seeded in WENRNicASY and WENRNicAST did not contain any goblet cells, and those seeded in WENRAT contained fewer goblet cells than those seeded in WENRAY (Figure S6). Unlike the colon cultures, no advantage in cell growth or TEER resulted from substitution of Y-27632 with thiazovivin in either duodenum (Figure S6) or ileum cultures. Therefore, further optimization of growth conditions focused on seeding cultures in WENRAY.

Similar to the strategy used for mouse small intestine cultures, global gene expression of human duodenum cultures was compared with that of duodenum tissue to optimize growth conditions. The Pearson correlation coefficient for gene expression of duodenum cultures seeded in WENRAY and differentiated with ENRA compared with that of duodenum tissue was highest when RNA was harvested from cultures on day 6, compared with days 3, 8, and 10 (Table S4). Moreover, duodenum cultures seeded in WENRAY and differentiated with either ENA or A83-01 showed better correlation with duodenum tissue than cultures differentiated with ENRA (Figure 4F). Therefore, the selected growth conditions for human small intestinal cultures were WENRAY in the seeding medium and ENA in the differentiation medium. The optimal monolayer growth conditions were successfully applied to duodenum cultures from all four patients tested.

Immunostaining for absorptive, goblet, enteroendocrine, and Paneth cell lineages confirmed that all of these major small intestinal cell lineages were present in the monolayer (Figure 4G). Quantification of cell lineage marker gene expression was consistent with the presence of all major intestinal cell lineages in the small intestine and colon cultures, although duodenum cultures had relatively lower expression of *CHGA* and *MUC2* compared with duodenal tissue (Figure S7). Many of the most differentially expressed genes observed in comparisons of duodenum, ileum, and distal colon tissue also showed consistent differential expression in the duodenum, ileum, and distal colon monolayer cultures, and the cultures clustered unsupervised with the intestinal tissue segment of origin, indicating that the cultures maintained segment-specific gene expression patterns (Figure 4H; Table S5). Several of the most differentially expressed genes from this gene expression list used to define intestinal segment-specific gene expression are shown in Figure 4I.

The optimized medium conditions for both mouse and human intestine monolayer cultures are summarized in Table 1.

Functional Evaluation of Human Monolayer Cultures

To further evaluate the function of the human monolayer cultures, a set of pharmacologically active compounds with known biological responses were tested. Forskolin elevates intracellular cAMP through activation of adenylyl cyclase, and can be used to elicit secretion of hormones from enteroendocrine cells (Nikoulina et al., 2010). To test the functional response of enteroendocrine and

Figure 4. Development and Characterization of Human Intestine Monolayer Cultures

(A) Human distal colon cultures actively transport sodium, potassium, and chloride ions following differentiation. Apical ion concentrations were measured for cultures seeded/differentiated (day 3) under different medium conditions. Fresh medium was added on day 5 and samples were collected on day 6 (20-hr incubation). Mean ± SD, n = 3. $p < 0.001$ for all differentiation conditions versus medium control. Representative of at least three experiments.

(B) Immunostaining for major cell lineages in distal colon cultures.

(C) Comparison of ion transporter expression in cultured cells and tissue from the proximal and distal colon. Average of two replicate experiments of triplicate wells.

(D) Relative mRNA expression in differentiated versus undifferentiated human distal colon cultures for a set of marker genes characteristic of differentiated distal colon cells. Mean ± SD.

(E) Relative mRNA expression in undifferentiated versus differentiated human distal colon cultures for a set of marker genes characteristic of undifferentiated colon cells. Mean ± SD.

(F) Pearson correlation coefficients for global gene expression profiles from duodenum cultures, derived from patients 11 and 13 and grown under different seeding and differentiation medium conditions, versus profiles from duodenum tissue samples from these patients.

(G) Immunostaining for major cell lineages of ileum cultures.

(H) Heatmap comparing gene expression in cultures versus tissue for duodenum, ileum, and distal colon using a list of genes with intestinal segment-specific expression (more than 5-fold enriched expression relative to the other intestinal segments; see Table S5).

(I) Several of the most differentially expressed intestine segment-specific genes from tissue plotted for human duodenum, ileum, and colon cultures; expression values were normalized to the segment with the highest expression level. Mean ± SD.

A, A83-01; E, epidermal growth factor; N, noggin; Nic, nicotinamide; R, R-spondin 1; S, SB202190; T, thiazovivin; W, Wnt3a; Y, Y-27632.

Table 1. Optimized Media Conditions for Differentiated Mouse and Human Intestine Monolayer Cultures

Intestinal Segment	Seeding Media	Growth Media	Differentiation Media
Mouse small intestine	$W_{2.5\times}$ENRY	$W_{2.5\times}$ENRY	ET + BMP-4
Mouse large intestine	WENRY	WENR	EN
Human small intestine	WENRAY	–	ENA
Human large intestine	WENRAT	–	ENRA

A, A83-01; BMP, bone morphogenetic protein; E, epidermal growth factor; N, noggin; R, R-spondin 1; T, thiazovivin; W, Wnt3a; Y, Y-27632.

enterochromaffin cells in human ileum monolayer cultures, cultures were treated with forskolin for 4 hr, and glucagon-like peptide 1 (GLP-1) and serotonin were measured in the basolateral medium. Both GLP-1 and serotonin were secreted in response to forskolin, demonstrating the presence of functional L cells and enterochromaffin cells in these cultures (Figure 5A).

The farnesoid X receptor (FXR) is a nuclear hormone receptor for bile acids that plays an important role in cholesterol and lipid homeostasis. Activation of FXR in the ileum elicits fibroblast growth factor 19 (FGF19) secretion into the portal circulation, which then acts in the liver to suppress bile acid synthesis (Kliewer and Mangelsdorf, 2015). We treated human ileum cultures with FXR agonist GW4064 for 4 hr and measured FGF19 secretion into the basolateral compartment. GW4064 elicited a concentration-dependent increase in FGF19 secretion into the basolateral chamber, indicating that bile acid signaling is intact in the human monolayer cultures (Figure 5B).

Aldosterone is an adrenal hormone that activates the mineralocorticoid receptor (MR) to regulate salt and water homeostasis. Activation of the MR in the distal colon has been shown to increase luminal sodium absorption through the upregulation of the epithelial sodium channel (ENaC) β and γ subunits (Bertog et al., 2008). Therefore, distal colon monolayers were treated with varying concentrations of aldosterone for 3 days and gene expression of the β subunit of ENaC was measured by qPCR. Aldosterone stimulated a concentration-dependent increase in ENaC β (*SCNN1B*) gene expression with a half maximal effective concentration of 130 pM (Figure 5C). Moreover, the apical volume of aldosterone-treated wells was significantly lower than control wells, confirming the functional increase in water absorption across the monolayer cultures (Figure 5D).

NHE3 (SLC9A3), as described above, is a sodium/hydrogen antiporter expressed in most intestinal segments that functionally absorbs luminal sodium in exchange for cellular protons. Tenapanor is a first-in-class, minimally absorbed small-molecule inhibitor of NHE3 (Spencer et al., 2014). Human ileum monolayers were treated with tenapanor overnight, and apical sodium concentration and pH were measured. Tenapanor produced a concentration-dependent decrease in sodium absorption from the apical to the basolateral compartment and inhibited apical proton secretion, both with a half maximal inhibitory concentration (IC_{50}) of 6 nM (Figures 5E and 5F). These findings are consistent with previously published potency values for tenapanor (Spencer et al., 2014).

Taken together, these results suggest that the optimized growth conditions yield human monolayer cultures that function as expected when treated with a range of well-characterized biologically active compounds.

Phenotype Screen of Mouse Distal Colon Monolayer Culture

To demonstrate the utility of intestinal organoids grown as monolayers for phenotype screening, we scaled the mouse distal colon monolayer cultures from 24- to 96-well plates and screened approximately 2,000 pharmacologically active compounds, covering a range of biological targets, for their ability to block K^+ absorption as a potential treatment for hyperkalemia. The compounds screened comprised those from the LOPAC1280 library and the Tocriscreen library; several inhibitors of Na^+/K^+-ATPase or gastric H^+/K^+-ATPase were also screened owing to the homology of these enzymes with colonic H^+/K^+-ATPase. While K^+ absorption in the distal colon cultures was the primary endpoint, TEER and apically applied rubidium transport measurements were used to counter-screen for compounds that block K^+ absorption via the loss of tight junction integrity (thereby preventing the cultures from establishing a K^+ gradient), rather than via inhibition of active K^+ transport. Vanadate (200 μM) was able to block K^+ absorption completely in the mouse distal colon cultures and was therefore chosen as a positive control to be included on each plate to monitor assay performance. Compounds were screened at a concentration of 30 μM in DMSO.

Inhibition of K^+ absorption was normalized to the mean value of vanadate controls on each plate such that a value of 1 indicated inhibition equivalent to vanadate. The mean ± SD inhibition for all compounds screened was 0.02 ± 0.25, for the DMSO negative controls it was 0.00 ± 0.17, and for the vanadate controls it was 1.00 ± 0.15. Compounds that inhibited K^+ absorption more than 3 SDs of the DMSO control (i.e., 0.50) were considered positive (Figure 6A). Compounds that inhibited K^+ absorption but reduced TEER and showed increased rubidium transport owing to paracellular leakage were discarded. The remaining positive compounds were screened an additional two times, and those that were confirmed

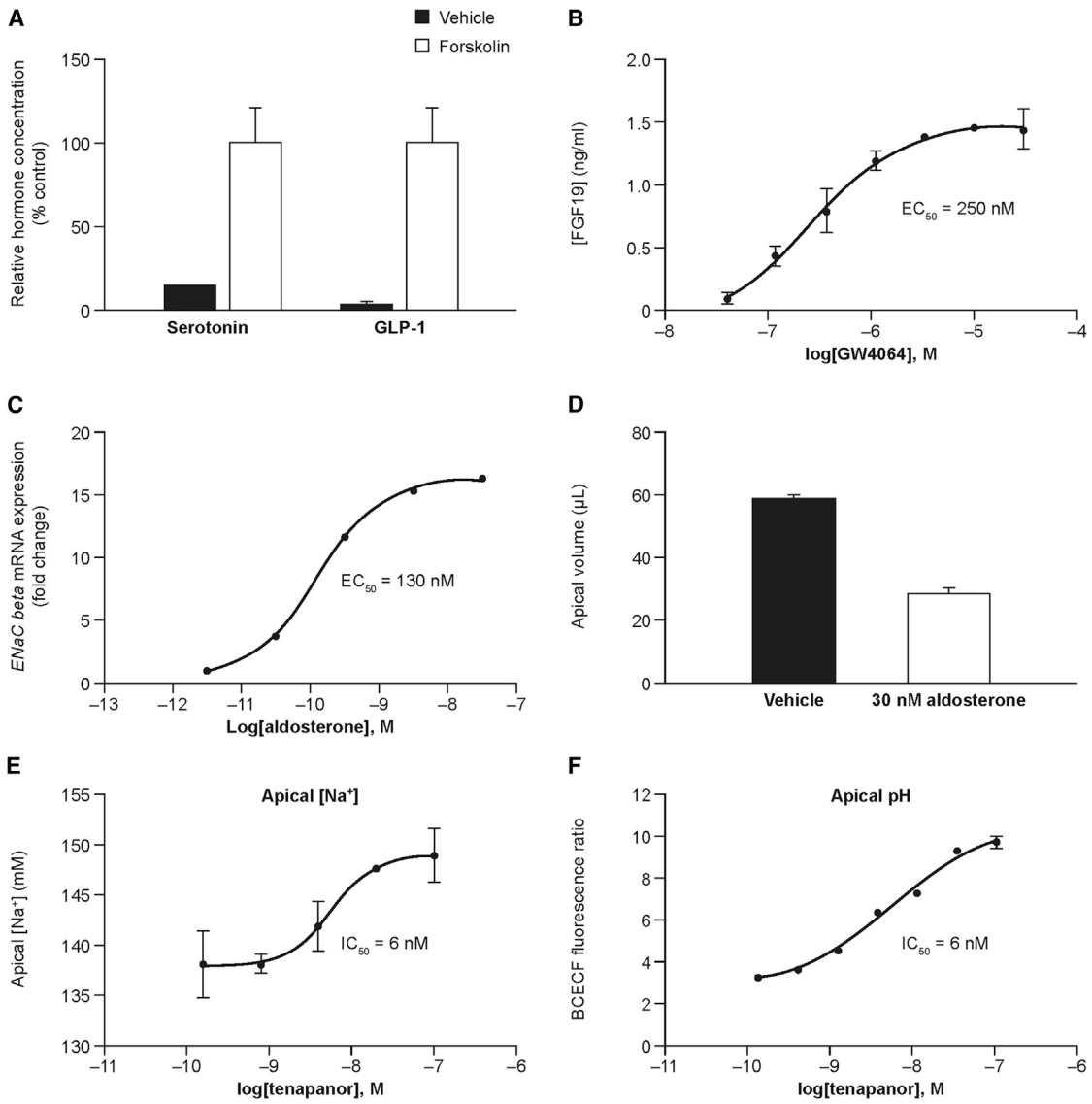

Figure 5. Functional Characterization of Human Cultures

(A) Serotonin and GLP-1 concentration in differentiated human ileum cultures treated with 100 µM forskolin or vehicle for 4 hr. Values for vehicle were normalized to forskolin response. Mean ± SD, n = 2. Representative of at least three experiments.

(B) FGF19 concentration in differentiated human ileum cultures treated with FXR agonist GW4064 for 4 hr. Mean ± SD, n = 2. Representative of at least three experiments.

(C) Expression of ENaC β chain mRNA in differentiated human distal colon cultures treated with aldosterone for 3 days. n = 2. Representative of at least two experiments.

(D) Apical volume of human distal colon cultures after 3 days of treatment with vehicle or 30 nM aldosterone. Initial apical volume was 200 µL. Mean ± SD, n = 2.

(E) Apical sodium concentration in differentiated human ileum cultures treated with tenapanor overnight (~16 hr). Mean ± SD, n = 2.

(F) Apical pH in differentiated human ileum cultures treated with tenapanor overnight (~16 hr). Mean ± SD, n = 2. Representative of at least three experiments.

positive (38 compounds) were further evaluated in concentration response.

Proscillaridin A (Figure 6B), a cardiac glycoside inhibitor of Na^+/K^+-ATPase, was among the most promising hits, first because it reproducibly inhibited K^+ absorption to a degree similar to vanadate without affecting TEER. Secondly, it was the only inhibitor within the set of Na^+/K^+-ATPase or gastric H^+/K^+-ATPase inhibitors tested, including ouabain

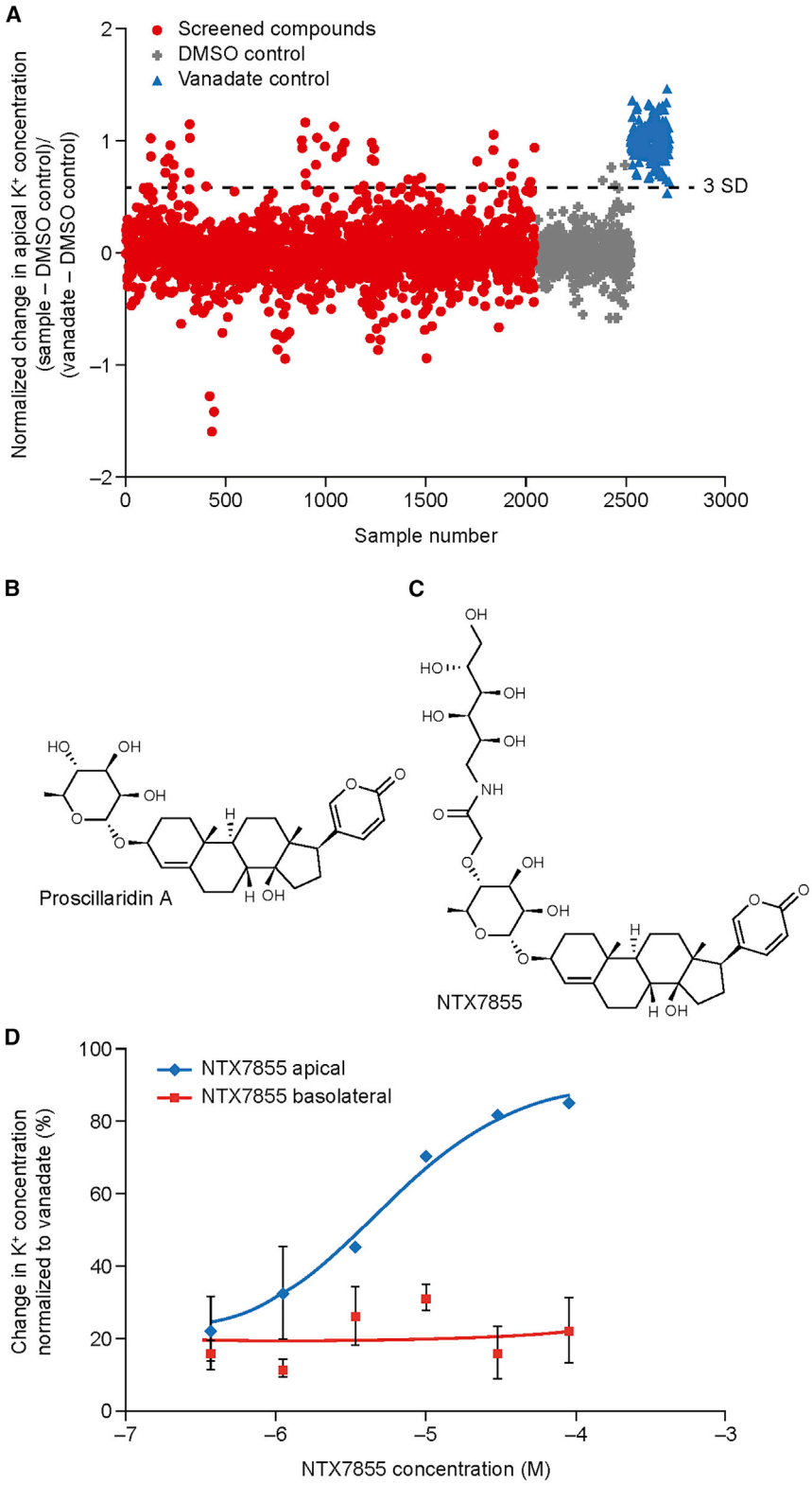

Figure 6. Compound Screen for Inhibition of Potassium Ion (K^+) Transport in Mouse Distal Colon Monolayer Cultures

(A) Compound screen at 30 μM for inhibition of K^+ transport from the apical to the basolateral compartments of mouse distal colon cultures. Data were normalized to DMSO (negative control) and vanadate (positive control), compounds that inhibited K^+ absorption greater than 3 SDs of the DMSO control were considered positive.

(B) Structure of proscillaridin A, a positive hit from the screen.

(C) Structure of NTX7855, a synthesized analog of proscillaridin A with reduced permeability.

(D) IC_{50} curves for inhibition of K^+ transport by NTX7855 applied to either the apical or the basolateral compartment of the cell culture plate. Mean ± SD, n = 3.

and SCH28080, which was positive. Thirdly, based on homology between colonic H^+/K^+-ATPase and Na^+/K^+-ATPase, it may be a direct inhibitor of mouse colonic H^+/K^+-ATPase that binds on the luminal side of the protein, a desirable property for a minimally absorbed drug (Laursen et al., 2013). To explore the properties of proscillaridin A further, an analog of this Na^+/K^+-ATPase inhibitor, NTX7855 (Figure 6C), was prepared with a polar moiety added to the glycoside to reduce cellular permeability. Administration of NTX7855 on the apical side of the mouse distal colon monolayer culture produced concentration-dependent inhibition of K^+ absorption with an IC_{50} of approximately 5 μM (Figure 6D). However, when NTX7855 was administered on the basolateral side of the monolayer, there was no inhibition of K^+ absorption, suggesting that the drug target was on the apical surface and consistent with the known apical localization of the colonic H^+/K^+-ATPase (Figure 6D). Furthermore, mass spectrometry indicated that permeability of the compound was low: its basolateral concentration was below the limit of detection (0.5 μM) 3 hr after 90 μM NTX7855 was administered on the apical side. Therefore, proscillaridin A and its less permeable analog NTX7855 were identified as inhibitors of active K^+ absorption in mouse distal colon cultures.

DISCUSSION

Intestinal organoid technology has proven to be a robust and valuable model system for studying intestinal epithelial cells and has advanced the understanding of intestinal epithelial cellular and molecular biology (Sato and Clevers, 2013). Here, we have demonstrated how optimization of culture conditions for growing intestinal epithelial cells as monolayers, as opposed to three-dimensional organoids, extends the utility of the platform by allowing unrestricted access to the apical and basolateral surfaces of the cultures, an essential characteristic to effectively study intestinal transport and secretion functions, and to enable the discovery and development of minimally systemic drugs with low cellular permeability.

Conditions for growing mouse colon monolayer cultures have been described previously (Moon et al., 2014). However, characterization of these cultures was limited to immunostaining for a small number of marker genes, making it difficult to determine whether these cultures maintained segment-specific gene expression patterns and functional phenotypes. These cultures did not distinguish proximal and distal colon and were differentiated using a γ-secretase inhibitor and lipopolysaccharide. Our experience with γ-secretase inhibitors suggests that the timing of addition is critical, and that this step provides a source of variability. Similar to mouse three-dimensional organoid cultures, the optimized mouse colon monolayer conditions we describe here do not require additional factors for differentiation, resulting in reproducible cultures that were scaled into 96-well plates and used to screen over 2,000 compounds. In addition, we observed significant gene expression and ion transport differences between proximal and distal mouse colon monolayer cultures, highlighting the importance of separating these two segments. Furthermore, we extend the mouse monolayer culture conditions to include all segments of the small intestine, where we found the addition of BMPs to be necessary for differentiation while maintaining monolayer integrity.

For human monolayer cultures, two different methods for growth and differentiation have been described, but characterization has been restricted to the assessment of only several marker genes without quantitative comparison with tissue expression levels, thus making it difficult to evaluate how similar these cultures are to their intestinal segment of origin (In et al., 2016; VanDussen et al., 2015). One method uses a mixture of Wnt3a, Noggin, and R-spondin1 (WRN medium) for growth and differentiation (VanDussen et al., 2015). Our results indicate that the presence of a TGF-β receptor (ALK4, 5, and 7) inhibitor (A83-01) is necessary for proper differentiation of monolayer cultures. The second method reported uses growth conditions similar to three-dimensional organoid growth conditions (WENRNicASY plus prostaglandin E2 and CHIR99021) for approximately 2 weeks, and differentiation is achieved 5 days after removing Wnt3a (In et al., 2016). Our results indicate that the presence of Nic and a p38 inhibitor (SB202190 [S]) significantly suppress secretory cell differentiation in monolayer cultures, consistent with previous findings in three-dimensional intestinal organoids (Sato et al., 2011). Using the WENRNicAS growth condition, we did not observe any goblet cells in our duodenal cultures, and there was a significant reduction in enteroendocrine cells in our ileum and colon cultures even after differentiation medium (ENRA) was applied. We also found that the timing of human monolayer culture growth and differentiation was important, and an optimal window was identified between days 5 and 7 of culture. Furthermore, we found that differentiating with ENA resulted in small intestine cultures that had better correlation of gene expression with freshly isolated tissue than did cultures differentiated with ENRA.

Our monolayer cultures enable direct measurement of ion transport across the intestinal epithelium. We show that cultures derived from different segments of the intestinal tract show different ion absorption rates and profiles, reflecting the segment-specific expression of ion transporters in the intestine. We have also established the monolayer model as a suitable system for studying the paracrine and endocrine secretory functions of the

intestine. We demonstrate the secretion of serotonin, the incretin hormone GLP-1, and the regulator of hepatic bile acid synthesis FGF-19, into the basolateral compartment of the monolayer cultures in response to the appropriate pharmacological stimuli.

We have demonstrated the use of our intestine monolayer platform in drug discovery by miniaturizing mouse distal colon monolayer cultures to 96-well plates, and conducting a phenotypic screen of approximately 2,000 compounds. The inhibitor of active K^+ absorption identified in the mouse distal colon cultures, NTX7855, provides proof of principle that this methodology can be used to discover inhibitors of ion transport. Such molecules may have potential as the basis for development of new therapeutics; for example, inhibitors of intestinal K^+ absorption may have utility in the treatment of patients with hyperkalemia.

EXPERIMENTAL PROCEDURES

A detailed description of all methods used is given in the Supplemental Information.

The process of isolating mouse intestinal crypts from the colon and small intestine was based on modifications of a published protocol and was approved by an institutional review board (Gracz et al., 2012). Human biopsies of intestinal tissue were obtained according to a protocol approved by the Copernicus Group Institutional Review Board (Durham, NC). Three-dimensional human intestinal organoid cultures were grown from biopsies and cultured for 7–12 days before being used to plate monolayer cultures (used up to passage 15) (Sato et al., 2011). Growth media and growth factors for mouse and human intestinal cultures were based on modifications of published protocols (Sato et al., 2009, 2011), and optimized growth conditions for monolayer cultures on Transwells are described in the Results section (Table 1) and the Supplemental Information.

RNA was isolated from monolayer cultures and from tissue using RNeasy kits (QIAGEN), and RNA libraries were prepared for sequencing using TruSeq Stranded RNA Library kits (Illumina). Transcript counts were obtained using the RNA Express application on the Illumina BaseSpace website. RNA profiles of cultures and tissue were compared by generating heatmaps and clustering using the heatmap.2 function in R, and Pearson correlation coefficients were determined in Microsoft Excel. Ion transport was determined by analyzing samples from the apical and basolateral chambers of each Transwell on an ion chromatography system (Thermo Fisher).

For the K^+ transport screening assay, mouse distal colon monolayer cultures were prepared in 96-well Transwell plates and used for assay on days 6, 7, or 8, depending on the TEER of the culture and its water-absorption phenotype. Wells with a TEER below 450 $\Omega \cdot cm^2$ were not used. Compounds were applied to the apical compartments and ion transport was assessed after 3 hr of incubation. The K^+ transport inhibitor NTX7855 was prepared from proscillaridin A, and characterized by proton nuclear magnetic resonance and mass spectrometry.

Statistics: in figure legends, "n" represents the number of independent replicate measurements made in an experiment. The p values were calculated using a two-tailed, unpaired t test.

ACCESSION NUMBERS

The accession number for the RNA sequencing data reported in this paper is GEO: GSE104803.

SUPPLEMENTAL INFORMATION

Supplemental Information includes Supplemental Experimental Procedures, seven figures, and five tables and can be found with this article online at https://doi.org/10.1016/j.stemcr.2017.10.013.

AUTHOR CONTRIBUTIONS

K.K., J.G.L., Z.Z., D.C., and M.S. designed experiments. K.K., Y.H., S.K.-McC., P.K., M.L., L.H., M.B., K.S., P.C., B.N., and M.S. performed experiments. M.S., A.J.K., and J.S.C. wrote the manuscript, with input from all authors. All authors approved the final manuscript for submission.

ACKNOWLEDGMENTS

This work was funded by Ardelyx. Editorial support was provided by Richard Claes of PharmaGenesis London, London, UK, funded by Ardelyx. K.K., Y.H., S.K.-M., P.K., M.L., L.H., J.G.L., A.J.K., J.S.C., and M.S. are employees of Ardelyx. P.C., K.S., B.N., Z.Z., and D.C. are former employees of Ardelyx. K.K., Y.H., S.K.-M., P.K., M.L., L.H., K.S., B.N., J.G.L., Z.Z., D.C., A.J.K., J.S.C., and M.S. are shareholders of Ardelyx.

Received: February 4, 2017
Revised: October 13, 2017
Accepted: October 15, 2017
Published: November 16, 2017

REFERENCES

Bertog, M., Cuffe, J.E., Pradervand, S., Hummler, E., Hartner, A., Porst, M., Hilgers, K.F., Rossier, B.C., and Korbmacher, C. (2008). Aldosterone responsiveness of the epithelial sodium channel (ENaC) in colon is increased in a mouse model for Liddle's syndrome. J. Physiol. *586*, 459–475.

Charmot, D. (2012). Non-systemic drugs: a critical review. Curr. Pharm. Des. *18*, 1434–1445.

Daniel, H. (2004). Molecular and integrative physiology of intestinal peptide transport. Annu. Rev. Physiol. *66*, 361–384.

Dawson, P.A., Lan, T., and Rao, A. (2009). Bile acid transporters. J. Lipid Res. *50*, 2340–2357.

Dekkers, J.F., Wiegerinck, C.L., de Jonge, H.R., Bronsveld, I., Janssens, H.M., de Winter-de Groot, K.M., Brandsma, A.M., de Jong, N.W., Bijvelds, M.J., Scholte, B.J., et al. (2013). A functional CFTR assay using primary cystic fibrosis intestinal organoids. Nat. Med. *19*, 939–945.

Farin, H.F., Jordens, I., Mosa, M.H., Basak, O., Korving, J., Tauriello, D.V., de Punder, K., Angers, S., Peters, P.J., Maurice, M.M., et al.

(2016). Visualization of a short-range Wnt gradient in the intestinal stem-cell niche. Nature *530*, 340–343.

Furness, J.B., Kunze, W.A., and Clerc, N. (1999). Nutrient tasting and signaling mechanisms in the gut. II. The intestine as a sensory organ: neural, endocrine, and immune responses. Am. J. Physiol. *277*, G922–G928.

Gracz, A.D., Puthoff, B.J., and Magness, S.T. (2012). Identification, isolation, and culture of intestinal epithelial stem cells from murine intestine. Methods Mol. Biol. *879*, 89–107.

Grun, D., Lyubimova, A., Kester, L., Wiebrands, K., Basak, O., Sasaki, N., Clevers, H., and van Oudenaarden, A. (2015). Single-cell messenger RNA sequencing reveals rare intestinal cell types. Nature *525*, 251–255.

In, J., Foulke-Abel, J., Zachos, N.C., Hansen, A.M., Kaper, J.B., Bernstein, H.D., Halushka, M., Blutt, S., Estes, M.K., Donowitz, M., et al. (2016). Enterohemorrhagic reduce mucus and intermicrovillar bridges in human stem cell-derived colonoids. Cell. Mol. Gastroenterol. Hepatol. *2*, 48–62.e3.

Jung, P., Sato, T., Merlos-Suarez, A., Barriga, F.M., Iglesias, M., Rossell, D., Auer, H., Gallardo, M., Blasco, M.A., Sancho, E., et al. (2011). Isolation and in vitro expansion of human colonic stem cells. Nat. Med. *17*, 1225–1227.

Kliewer, S.A., and Mangelsdorf, D.J. (2015). Bile acids as hormones: the FXR-FGF15/19 pathway. Dig. Dis. *33*, 327–331.

Kunzelmann, K., and Mall, M. (2002). Electrolyte transport in the mammalian colon: mechanisms and implications for disease. Physiol. Rev. *82*, 245–289.

Laursen, M., Yatime, L., Nissen, P., and Fedosova, N.U. (2013). Crystal structure of the high-affinity Na^+K^+-ATPase-ouabain complex with Mg^{2+} bound in the cation binding site. Proc. Natl. Acad. Sci. USA *110*, 10958–10963.

Merlos-Suarez, A., Barriga, F.M., Jung, P., Iglesias, M., Cespedes, M.V., Rossell, D., Sevillano, M., Hernando-Momblona, X., da Silva-Diz, V., Munoz, P., et al. (2011). The intestinal stem cell signature identifies colorectal cancer stem cells and predicts disease relapse. Cell Stem Cell *8*, 511–524.

Middendorp, S., Schneeberger, K., Wiegerinck, C.L., Mokry, M., Akkerman, R.D., van Wijngaarden, S., Clevers, H., and Nieuwenhuis, E.E. (2014). Adult stem cells in the small intestine are intrinsically programmed with their location-specific function. Stem Cells *32*, 1083–1091.

Moon, C., VanDussen, K.L., Miyoshi, H., and Stappenbeck, T.S. (2014). Development of a primary mouse intestinal epithelial cell monolayer culture system to evaluate factors that modulate IgA transcytosis. Mucosal Immunol. *7*, 818–828.

Nikoulina, S.E., Andon, N.L., McCowen, K.M., Hendricks, M.D., Lowe, C., and Taylor, S.W. (2010). A primary colonic crypt model enriched in enteroendocrine cells facilitates a peptidomic survey of regulated hormone secretion. Mol. Cell. Proteomics *9*, 728–741.

Sabbagh, Y., O'Brien, S.P., Song, W., Boulanger, J.H., Stockmann, A., Arbeeny, C., and Schiavi, S.C. (2009). Intestinal npt2b plays a major role in phosphate absorption and homeostasis. J. Am. Soc. Nephrol. *20*, 2348–2358.

Sangan, P., Rajendran, V.M., Mann, A.S., Kashgarian, M., and Binder, H.J. (1997). Regulation of colonic H-K-ATPase in large intestine and kidney by dietary Na depletion and dietary K depletion. Am. J. Physiol. *272*, C685–C696.

Sato, T., and Clevers, H. (2013). Growing self-organizing mini-guts from a single intestinal stem cell: mechanism and applications. Science *340*, 1190–1194.

Sato, T., Stange, D.E., Ferrante, M., Vries, R.G., Van Es, J.H., Van den Brink, S., Van Houdt, W.J., Pronk, A., Van Gorp, J., Siersema, P.D., et al. (2011). Long-term expansion of epithelial organoids from human colon, adenoma, adenocarcinoma, and Barrett's epithelium. Gastroenterology *141*, 1762–1772.

Sato, T., Vries, R.G., Snippert, H.J., van de Wetering, M., Barker, N., Stange, D.E., van Es, J.H., Abo, A., Kujala, P., Peters, P.J., et al. (2009). Single Lgr5 stem cells build crypt-villus structures in vitro without a mesenchymal niche. Nature *459*, 262–265.

Seidler, U., Song, P., Xiao, F., Riederer, B., Bachmann, O., and Chen, M. (2011). Recent advances in the molecular and functional characterization of acid/base and electrolyte transporters in the basolateral membranes of gastric and duodenal epithelial cells. Acta Physiol. (Oxf.) *201*, 3–20.

Spencer, A.G., Labonte, E.D., Rosenbaum, D.P., Plato, C.F., Carreras, C.W., Leadbetter, M.R., Kozuka, K., Kohler, J., Koo-McCoy, S., He, L., et al. (2014). Intestinal inhibition of the Na^+/H^+ exchanger 3 prevents cardiorenal damage in rats and inhibits Na^+ uptake in humans. Sci. Transl. Med. *6*, 227ra236.

Sun, H., Chow, E.C., Liu, S., Du, Y., and Pang, K.S. (2008). The Caco-2 cell monolayer: usefulness and limitations. Expert Opin. Drug Metab. Toxicol. *4*, 395–411.

Talbot, C., and Lytle, C. (2010). Segregation of Na/H exchanger-3 and Cl/HCO_3 exchanger SLC26A3 (DRA) in rodent cecum and colon. Am. J. Physiol. Gastrointest. Liver Physiol. *299*, G358–G367.

van de Wetering, M., Francies, H.E., Francis, J.M., Bounova, G., Iorio, F., Pronk, A., van Houdt, W., van Gorp, J., Taylor-Weiner, A., Kester, L., et al. (2015). Prospective derivation of a living organoid biobank of colorectal cancer patients. Cell *161*, 933–945.

VanDussen, K.L., Marinshaw, J.M., Shaikh, N., Miyoshi, H., Moon, C., Tarr, P.I., Ciorba, M.A., and Stappenbeck, T.S. (2015). Development of an enhanced human gastrointestinal epithelial culture system to facilitate patient-based assays. Gut *64*, 911–920.

Yui, S., Nakamura, T., Sato, T., Nemoto, Y., Mizutani, T., Zheng, X., Ichinose, S., Nagaishi, T., Okamoto, R., Tsuchiya, K., et al. (2012). Functional engraftment of colon epithelium expanded in vitro from a single adult Lgr5(+) stem cell. Nat. Med. *18*, 618–623.